*Conference on Modelling Fluid Flow (CMFF'12)*
*The 15th International Conference on Fluid Flow Technologies*
*Budapest, Hungary, September 4-7, 2012*

# CFD MODELLING FOR PERFORMANCE PREDICTIONS OF A HYDRAULIC TURBINE DRAFT TUBE: THE EFFECT OF INLET BOUNDARY CONDITIONS FOR TWO-EQUATION TURBULENCE MODELS

Anton B. KORSAKOV[1], Evgueni M. SMIRNOV[1], Valery D. GORYACHEV[2]

[1] Department of Aerodynamics, St.-Petersburg State Polytechnic University. E-mail: aero@phmf.spbstu.ru
[2] Corresponding Author. Department of Mathematics, Tver State Technical University. 170026, Tver, Russia. Tel.: +7 4822 311510, E-mail: valery@tversu.ru

## ABSTRACT

Turbulent flow in an elbow draft tube of an axial turbine is calculated with an in-house CFD-code on the base of the RANS approach. The focus is to study sensitivity of the predicted pressure recovery and outlet energy non-uniformity to wide variations in the inlet boundary conditions for transported turbulence quantities used in popular turbulence models, such as the standard $k$-$\varepsilon$ model, the Wilcox $k$-$\omega$ model and the Menter SST model. This information is important for appropriate CFD-based optimization. The steady-state computations at the inlet Reynolds number of about $6 \cdot 10^5$ were performed for a draft tube with two outlet channels tested several decades ago at an air test rig in combination with a runner. At the computations, inlet distributions of three velocity components were fixed and defined by experimental profiles. It has been established that in case of the $k$-$\varepsilon$ and the $k$-$\omega$ model the engineering quantities characterizing the draft tube performance change dramatically when the inlet turbulent-to-molecular viscosity ratio are gradually increased from 100 to 10,000, with the inlet turbulence intensity varied from 5% to 10%. The SST model shows a considerably weaker sensitivity despite it produces a more complicated flow field. A comparison with the measurement data is given.

**Keywords: CFD, draft tube flow, axial hydraulic turbine, turbulence modelling**

## NOMENCLATURE

| | | |
|---|---|---|
| $A$ | $[m^2]$ | cross section area |
| $D$ | $[m]$ | diameter |
| $K$ | [-] | non-uniformity factor of the outlet dynamic pressure |
| $Q$ | $[m^3/s]$ | flow rate |
| $R$ | $[m]$ | radial distance from the runner axis |
| $Re$ | [-] | Reynolds number |
| $S$ | $[1/s]$ | strain tensor magnitude |
| $Tu$ | [-] | inlet turbulence intensity |
| $U$ | $[m/s]$ | bulk velocity |
| $\underline{V}$ | $[m/s]$ | velocity vector |
| $V_n$ | $[m/s]$ | normal velocity at a cross section |
| $V_z, V_r, V_t$ | $[m/s]$ | axial, radial and circumferential velocity components |
| $Y^+$ | [-] | normalized distance to the wall of the first calculation point |
| $X, Y, Z$ | $[m]$ | Cartesian coordinates |
| $k$ | $[m^2/s^2]$ | turbulent kinetic energy |
| $p$ | $[Pa]$ | pressure |
| $q$ | $[Pa]$ | mass-averaged dynamic pressure |
| $\varepsilon$ | $[m^2/s^3]$ | dissipation rate of turbulent kinetic energy |
| $\eta$ | [-] | pressure recovery factor |
| $\nu$ | $[m^2/s]$ | molecular kinematic viscosity |
| $\nu_t$ | $[m^2/s]$ | turbilent viscosity |
| $\rho$ | $[kg/m^3]$ | density |
| $\omega$ | $[1/s]$ | turbulence eddy frequency |

**Subscripts and Superscripts**

| | |
|---|---|
| in | at the inlet of the draft tube |
| out | at the outlet of the draft tube |
| $t$ | turbulent |

## 1. INTRODUCTION

The task of a hydraulic draft tube is to convert the kinetic energy of the fluid leaving the turbine runner to a static pressure rise. Consequently, minimizing the energy losses is a challenge in the design of draft tubes. The relative importance of the losses depends on the water head. Particularly in case of the low head power plants, the losses in the draft tubes become relatively large and the design or redesign of existing draft tubes prove to be a critical issue.

In essence, the draft tube is a diffuser that typically has a complicated form, especially in the

elbow draft tube case. The diffuser nature of the draft tube flow predefines a strong influence of the inlet conditions, depending in turn on the regime of runner operation. Generally, the flow entering the draft tube can be characterized as three dimensional, turbulent and swirling.

Many Computational Fluid Dynamics (CFD) studies are dealing with the complex flow in the elbow draft tubes. A great deal of effort has been made in 1999-2005 by numerous participants of the ERCOFTAC Turbine-99 Workshops [1,2] at test computations of the flow in the sharp-heel draft tube of a Kaplan hydraulic turbine model studied at the Alvkarleby laboratory in Sweden. The computations were performed on the base of steady-state or unsteady problem formulation with various commercial and in-house CFD-codes using a number of turbulence models for closing the Reynolds-averaged Navies-Stokes (RANS) equations. Attempts of Large Eddy Simulation (LES) were presented at the 3rd Workshop as well. As an important result of these test calculations, it was stated that apart from discretization errors and specifics of a particular turbulence model the flow structure and the pressure field, as well as the engineering quantities predicted, are rather sensitive both to the inlet distributions of mean velocity components and to values prescribed at the draft tube inlet for transported turbulence quantities (see, for instance, [3]).

A straight way to overcome this issue is to simulate the flow through a whole rotor/stator configuration including stay vanes, guide vanes, a runner and a draft tube. Such kind of time and resource consuming computations are performed for models of the Francis turbines, with the aim to predict unsteady flow phenomena responsible for arising high pressure pulsations, first of all due to formation of the known vortex rope during partial load operation of the turbine [4-6]. However, adequate prediction of turbulence at the runner exit of a Kaplan turbine potentially can be achieved only at very cost unsteady rotor/stator calculations that would be able to resolve the vane wakes (interacting with the runner) and the runner blade wakes. Consequently, this “straight-way” approach hardly might be applied for engineering purposes in the near future, including a desire (see, for instance, [7-8]) to get tools for automatic shape optimization of draft tubes for low head hydraulic turbines.

Recently De Henau et al. [9] reported an investigation of methodologies to improve the reliability of CFD RANS-based analysis of axial turbine draft tubes. The study was performed with the ANSYS CFX 12.0 software using the SST turbulence model [10]. A steady-state rotor/stator solution (obtained with the mixing-plane approximation) and a draft tube only solution are presented. Particularly it has been established that in case of the draft tube only simulation prescribing a circumferential average value of the turbulent kinetic energy together with an average turbulent length scale as turbulence inlet conditions for the SST model equations is a proper technique as long as these averages are coherent with the rotor/stator steady solution. Nevertheless, comparisons of simulation results with the experimental data highlight some discrepancies between the predicted draft tube flow and the experimental observations.

All the above mentioned gives a motivation to study sensitivity of prediction results for the draft tube performance to wide variations in the inlet boundary conditions for transported turbulence quantities used in RANS turbulence models. The present contribution covers results of such a study for three two-equation turbulence models. The computations were performed for the axial turbine draft tube model examined many years ago at a large-scale air test rig that was under extensive operation at the Department of Aerodynamics of the Leningrad Polytechnic Institute (LPI, currently the St.-Petersburg State Polytechnic University) in the fifties of the last century.

## 2. TEST CASE

### *2.1. Experimental configuration*

Figure 1 shows a scheme of the LPI aero test rig that was assembled in the middle of the last century to examine models of axial turbines. This rig was extensively used for many years to provide experimental data for performance of turbines designed for several hydro power plants in Russia.

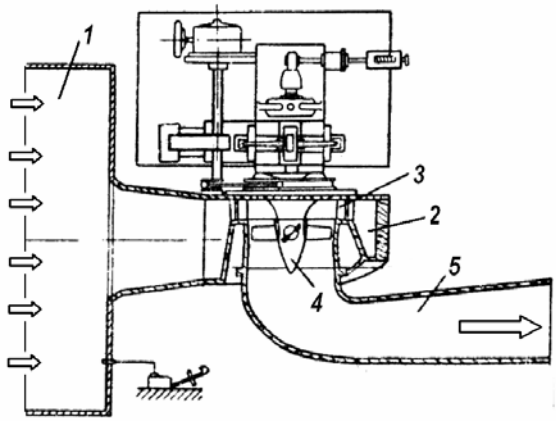


**Figure 1. Scheme of the LPI aero test rig: (1) delivery duct, (2) spiral chamber, (3) guide vanes, (4) runner, (5) draft tube**

The particular case selected for the present study is one of the variants of the draft tube design for the Kuibyshev hydroplant. Generally, this test case is described in [11], additional details were taken from available internal reports.

The draft tube under consideration consists of a short conical diffuser followed by a strongly curved

90º elbow of a varying cross section (circular to rectangular) and then by two outlet channels separated by a pier (Figures 2,3). The outer diameter of the draft tube inlet section, $D_{in}$, is 434 mm. The outlet-to-inlet expansion ratio of the draft tube is of 4.88. Other dimensions characterizing the draft tube geometry are given in Fig.2.

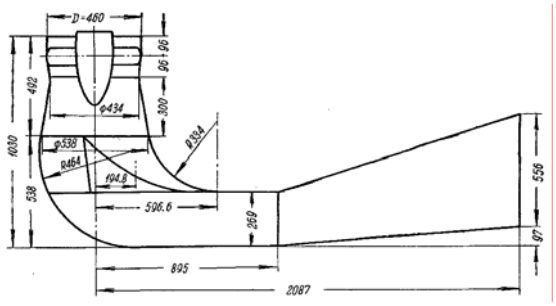


**Figure 2. Dimensions of the test draft tube**

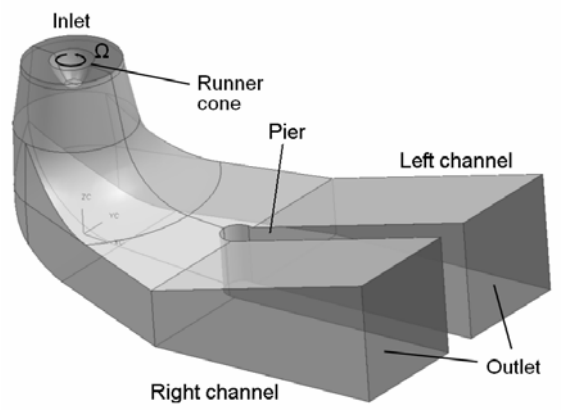


**Figure 3. 3D model of the test draft tube**

At the selected measurements of the draft tube flow, the runner, 460 mm diameter, with the blade angle of incidence of 15°, rotated with the angular speed of 2553 revolution per minute. The flow rate was kept at 2.64 $m^3/s$, that gave the inlet Reynolds number, $Re=U_{in}\cdot D_{in}/\nu$, of about $6\cdot10^5$. The draft tube outlet was open directly to atmosphere.

### 2.2. Measurement data

Three components of the velocity and the local static pressure were measured at the inlet and outlet sections of the draft tube using a spherical five-hole probe. The inlet velocity profiles were measured along one radial direction. The results given in [11] for the inlet section are reproduced in Figure 4.

For evaluation of the draft tube performance, two engineering quantities were calculated via integration of the measured velocity and pressure distributions over the inlet and outlet sections. The first one is the pressure recovery factor

$$\eta = < \Delta p > / q_{in} \qquad (1)$$

where the mass-averaged pressure rise, $<\Delta p>$, and the inlet dynamic pressure, $q_{in}$, are defined by

$$< \Delta p >= Q^{-1} \int_{A_{in}} ( p_{out} - p_{in} ) V_n dA \qquad (2)$$

$$q_{in} = Q^{-1} \int_{A_{in}} \frac{\rho V^2}{2} V_n dA \qquad (3)$$

In Eq.(2) the outlet static pressure, $p_{out}$, was treated in as a constant equal to the atmospheric one.

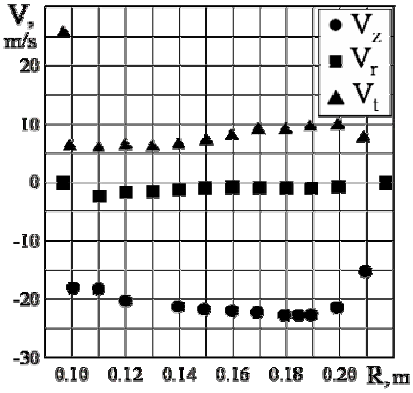


**Figure 4. Experimental velocity component profiles at the draft tube inlet**

The second integral quantity, $K$, is the non-uniformity factor of the outlet dynamic pressure. It is evaluated as

$$K = \left( Q \frac{\rho U_{out}^2}{2} \right)^{-1} \int_{A_{out}} \frac{\rho V^2}{2} V_n dA \qquad (4)$$

As reported in [11], for the test case selected, η=0.60, and K=4.07.

## 3. COMPUTATIONAL ASPECTS

### 3.1. Mathematical formulation

The present computations are performed on the base of the incompressible fluid Reynolds-averaged Navier-Stokes equations written for the case of steady-state mean flow. To close the RANS equations, two-equation turbulence models based on the isotropic turbulent viscosity assumption are used in combination with techniques of enhanced wall function. Among the wide variety of models of this family, the following three have been chosen due to their popularity in the CFD community: the standard $k$-$\varepsilon$ model (written with the Kato-Launder modification [12]), the Wilcox $k$-$\omega$ model [13] and the Menter SST model. The latter is applied in the formulation given in [10].

In case of the $k$-$\varepsilon$ model, enhanced wall functions suggested and validated in [14] are used. These functions produce good quality results for the near wall layer even if $Y^+$ for the computational grid used is as low as 3-4. For the Wilcox $k$-$\omega$ model and the SST model, an approach similar to that suggested in [15] for the 'automatic wall treatment' is applied.

### 3.2. Boundary conditions

Boundary conditions are specified at the inlet, outlet and solid wall boundaries of the draft tube model. Inflow boundary conditions are prescribed at the start of the conical diffuser using interpolation of the measured mean axial, circumferential and radial velocity profiles (shown in Fig. 4). Due to lack of more detailed data, the calculations were carried out assuming that the inlet flow is axisymmetric.

The inlet turbulence is specified by prescribing turbulence intensity, $Tu$, and the turbulent-to-molecular viscosity ratio, $(\nu_t/\nu)_{\text{in}}$. To define inlet values of the transported turbulence quantities the following relations are used

$$k_{in} = \frac{3}{2}\left(Tu \cdot U_{in}\right)^2 \tag{5}$$

$$\varepsilon_{in} = \left(C_\mu k_{in}^2/\nu\right)/\left(\nu_t/\nu\right)_{in} \tag{6}$$

$$\omega_{in} = \left(k_{in}/\nu\right)/\left(\nu_t/\nu\right)_{in} \tag{7}$$

where $C_\mu$=0.09 is an empirical constant of the $k$-$\varepsilon$ model. At the calculations, the inlet turbulence intensity was set to 5%, 7.5%, or 10%, while the inlet viscosity ratio was varied from 100 to 10,000.

For pressure, the homogeneous Neumann boundary condition was used everywhere except at the outlet, where the area-averaged pressure is set to zero. Recirculating flow allowed at the outlet, with the homogeneous Neumann boundary condition where the flow was directed outward, and constant values of the turbulence transported quantities (coherent with the inlet values) where recirculation occurred.

### 3.3. Computational grid

A block-structured grid of about 150 K nodes was generated for the calculations. The grid is symmetrical with respect to the middle plane. Half of the grid is illustrated in Figure 5. The solutions presented below yielded first-computational-point wall distances of $5< Y^+ <80$ with an appropriate average of $Y^+$=30.

Sure, today such a grid may be treated as a relatively coarse one. However, this choice was motivated by the following considerations. First, it is no much sense to perform refined CFD modeling under conditions of existing experimental uncertainties related to the mean velocity distributions over the inlet, when there is no information about variations of the inlet velocity along the circumferential direction, and resolution of the near wall layers is pure. Second, it is well known that using a refined grid might result in problems of getting a steady-state solution for such a complicated three-dimensional flows, and the need to perform time-consuming unsteady computations is extremely undesirable for extensive parametric computations.

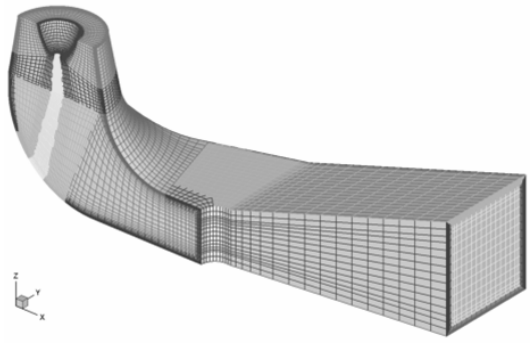

**Figure 5. Half of the computational grid**

### 3.4. CFD code

The calculations were performed with the in-house code SINF being under long-time development at the Department of Aerodynamics of the St.-Petersburg State Polytechnic University. This 3D incompressible/compressible Navier-Stokes code is based on the second-order finite-volume spatial discretization using the cell-centered variable arrangement and body-fitted block-structured grids. A general description of the code capabilities is given by Smirnov and Zajtsev [16]. One of the examples of refined simulations of 3D turbulent flows performed with this code and comparisons with the ANSYS CFX software results are given in [17].

## 4. RESULTS

### 4.1. Flow visualization

Figure 6 illustrates typical flow patterns computed for the draft tube under consideration with three different turbulence models. One can see that the $k$-$\varepsilon$ model and the Wilcox model yield very similar results for global flow structure, with a relatively low intensity of the vortex forming in the elbow region and entering then into the left outlet channel. Contrary to that, the SST model produces a rather intensive vortex in the left outlet channel, and a pronounced swirl in the right channel as well. From a detailed flow analysis one can conclude that a more complicated structure of the flow predicted with the SST model is due to a several times lower

level of the flow core turbulent viscosity, as compared with the fields predicted by the other two turbulence models. Obviously, this reduction of the flow core turbulent viscosity is a result of the limitation introduced by Menter into the expression defining this quantity,

$$\nu_t = \frac{0.31k}{max(0.31\omega, SF_2)}, \qquad (8)$$

where $S$ is the mean flow strain rate, and $F_2$ is one of the empirical functions of the SST model [10].

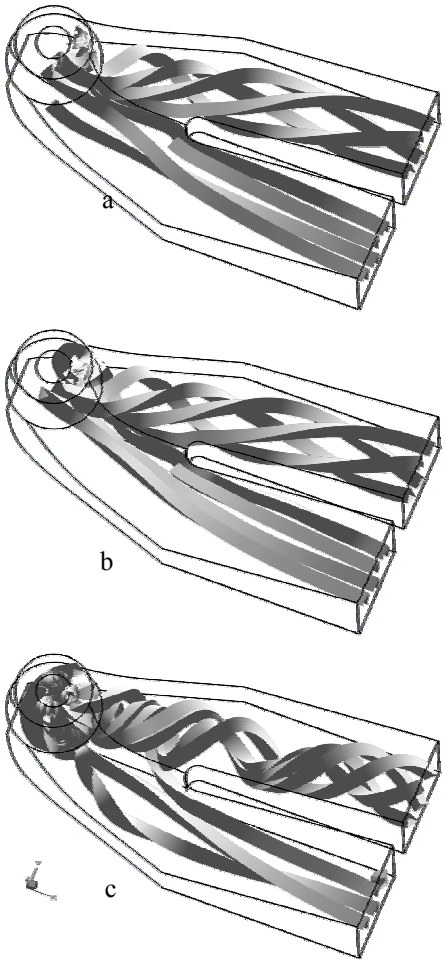


**Figure 6. Streamline patterns computed with (a) *k-ε* , (b) *k-ω*, and (c) SST turbulence model**

Figure 7 presents an example of streamwise velocity distributions over the outlet section, $Tu$=5%, $(\nu_t/\nu)_{in}=10^3$. One can see a pronounced unbalance of flows leaving the draft tube through the right and the left channels. From the other side, for all the tubulence models used, the right channel flow (more intensive) is highly non-uniform, with a maximum shifted to the side-bottom corner. Most distictions between the patterns obtained for different turbulence models are observed at the outlet of the left channel. For instance, a local minimum in the flow core is seen in the SST model case whereas for two other models the velocity varies steadily from the bottom to the top.

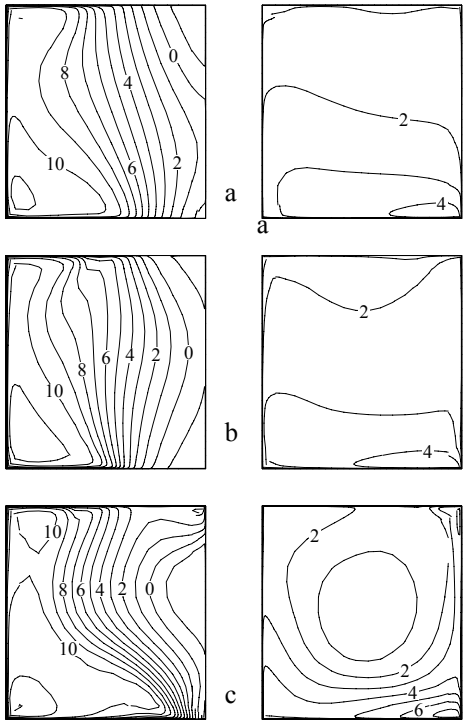


**Figure 7. Outlet streamwise velocity distributions computed at $Tu$=5% and $(\nu_t/\nu)_{in}=10^3$ with (a) *k-ε* , (b) *k-ω*, and (c) SST turbulence model**

### *4.2. Engineering quantities*

Effect of wide variations in the inlet turbulence parameters on the predicted pressure recovery and outlet energy non-uniformity is illustrated in Figures 8,9. It is clearly seen that in case of the *k-ε* and the Wilcox *k-ω* model the engineering quantities characterizing the draft tube performance change strongly over the whole range of the inlet viscosity ratio variations. The effect of an inlet turbulence intensity increase is more pronounced in the *k-ε* case. When comparing the prediction results with the experimental data one can conclude that the Wilcox *k-ω* model data match the experiments at $(\nu_t/\nu)_{in}$ of about $10^3$. However this result should be treated as a casual one.

The SST turbulence model shows a weaker sensitivity to variations in the viscosity ratio especially for the outlet energy non-uniformity factor, the predicted value of which is in a surprisingly well agreement with the experimental data. The pressure recovery factor yielded by the SST model turns to be more sensitive to the inlet turbulence intensity variations, and it is typically under-predicted as compared with the measurements. However, for the highest value of $Tu$ and $(\nu_t/\nu)_{in}>10^3$ the calculation and the experimental data are in a satisfactory agreement.

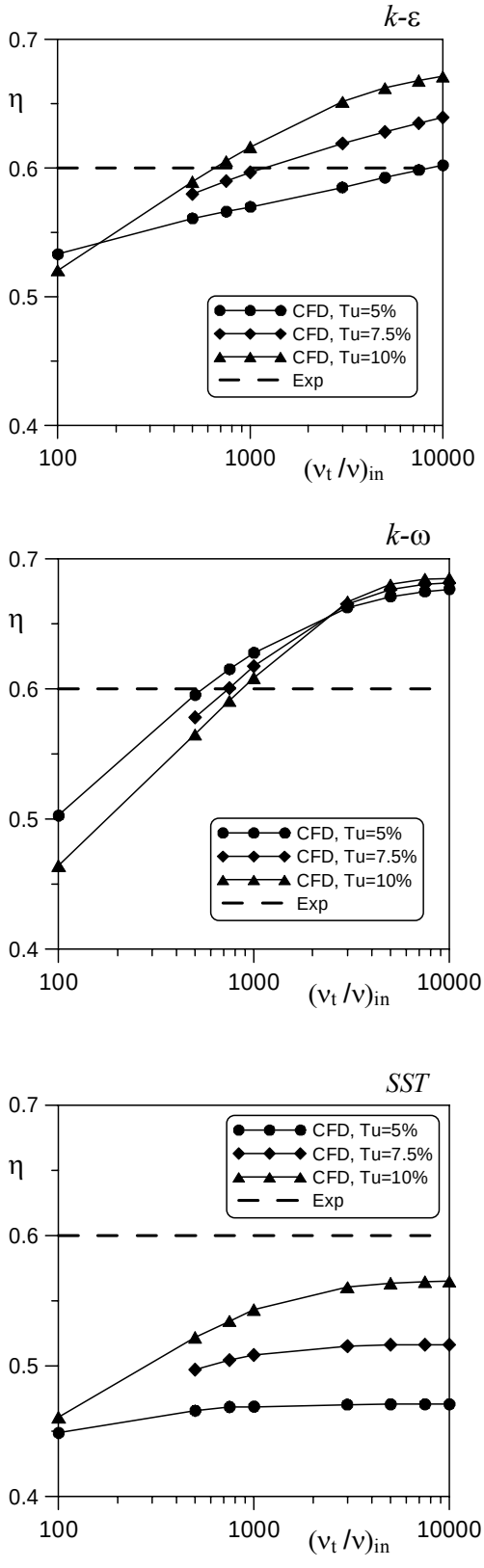


**Figure 8. Effect of turbulence inlet boundary conditions on the pressure recovery factor computed with (top) *k-ε* , (middle) *k-ω*, and (bottom) SST turbulence model**

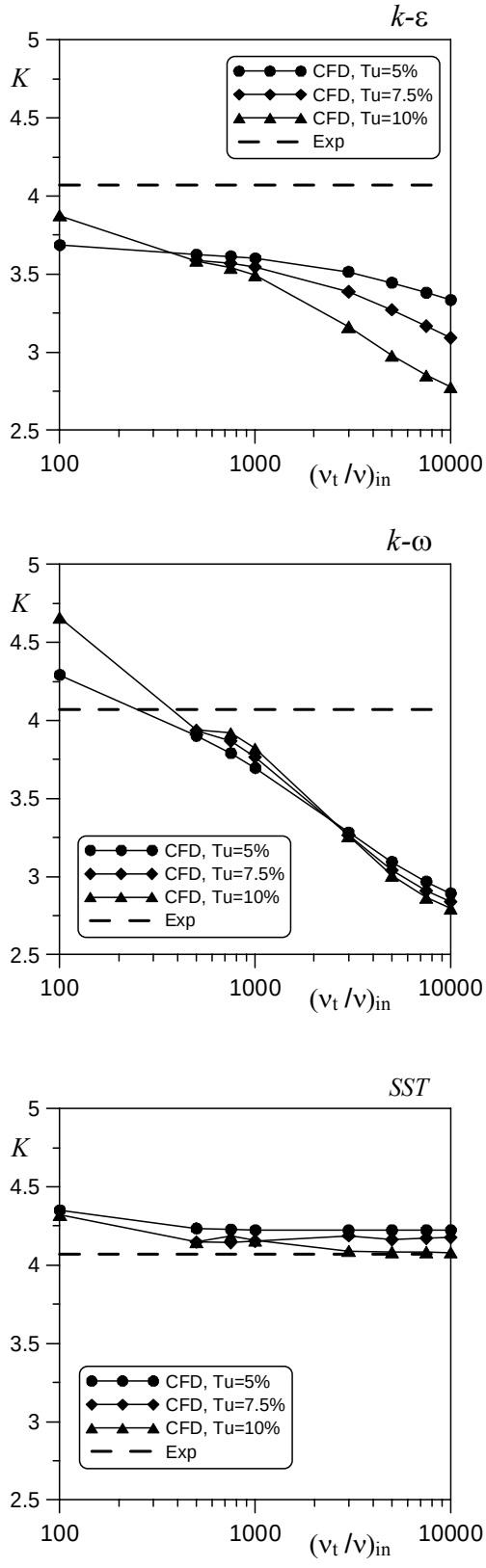


**Figure9. Effect of turbulence inlet boundary conditions on the outlet dynamic pressure non-uniformity factor computed with (top) *k-ε* , (middle) *k-ω*, and (bottom) SST turbulence model**

## 5. SUMMARY

Systematic RANS-based computations have been performed for an axial turbine elbow draft tube using fixed prescribed profiles of the inlet velocity components and widely varied inlet values of turbulence quantities. The inlet turbulence intensity was in the 5% to 10% range while the inlet turbulent-to-molecular viscosity ratio was varied from 100 to 10,000. The standard $k$-$\varepsilon$ turbulence model and the Wilcox $k$-$\omega$ model predict the engineering quantities, which change dramatically with inlet turbulence variations. Generally, the SST model shows a weaker sensitivity despite it produces a more complicated flow field as compared with the two other models. It should be treated as an attractive feature of the SST model having in mind developments of tools for automatic CFD-based shape optimization of the draft tubes, at least for low head hydraulic turbines.

## REFERENCES


[1] Engström T.F., Gustavsson H., Karlsson R. I., 2002, "Turbine-99 – Workshop 2 on Draft Tube Flow", Proc. *21st IAHR Symposium on Hydraulic Machinery and Systems,* Laussane, Switzerland.

[2] Cervantes M. J., Engström T. F., Gustavsson L. H., 2005, "Turbine-99 III", Proc. *3rd IAHR/ERCOFTAC Workshop on Draft Tube Flow,* Porjus, Sweden.

[3] Page, M., Giroux, A.-M., Nicolle, J., "Steady and unsteady computations of Turbine 99 draft tube", Proc. *3rd IAHR/ERCOFTAC workshop on Draft Tube Flow, Turbine99-III*, Porjus, Sweden, Paper No. 9

[4] Ruprecht, A., Maihöfer, M., Heitele, M., and Helmrich, T., 2002, "Massively parallel computation of the flow in hydro turbines," Proc. *21st IAHR Symposium on Hydraulic Machinery and Systems*, Lausanne, Switzerland, pp. 199–206.

[5] Ciocan, D., Iliescu, M.,S., Vu, T.,C., Nennemann, B., Avellan, F., 2007, "Experimental study and numerical simelation of the FLINDT draft tube rotating vortex", *ASME J Fluid Eng*., Vol.129, pp.146-158.

[6] Magnoli, M. V., Schilling, R., 2008, "Vortex shedding in Francis runners trailing edges", Proc. *24th IAHR Symposium,* Foz do Iguaçu, Brazil.

[7] Eisinger, R., Ruprecht, A., 2005, "Automatic shape optimization of hydro turbine components based on CFD", Proc. *Workshop on Turbomachinery Hydrodynamics*, Timisoara, Romania.

[8] Marjavaara, B.D, Lundström, T. S, 2006, "Redesign of a sharp heel draft tube by a validated CFD-optimization", *Int. J Numer. Meth. Fluids,* Vol. 50, pp. 911-924.

[9] De Henau, V., Payette, F.-A, Sabourin, M., Gagnon, J-M., Gouin, P., Deschênes, C., 2010, "Computational study of a low head draft tube and validation with experimental data", Proc. *25th IAHR Symposium on Hydraulic Machinery and Systems,* Timisoara, Romania.

[10] Menter, F.R., Langtry R., Kuntz M., 2003, "Ten years of industrial experience with the SST turbulence model", *Turbulence, Heat and Mass Transfer 4 (CD-ROM Proceedings).* Begell House, Inc.

[11] Nevsky, D.Y., Sinochkina, L.A., 1955, "Study of the draft tube of a hydraulic turbine model for the Kuibyshev hydroplant", *Trans. Leningrad Polytechnic Institute*, No. 176, pp. 76-91 (in Russian).

[12] Kato, M., Launder, B.E., 1993, "The modelling of turbulent flow around stationary and vibrating square cylinders", Proc. *9th Symposium on Turbulent Shear Flows,* Kyoto, Japan, pp. 1041-1046.

[13] Wilcox, D., 1988, "Reassessment of the scale-determining equation for advanced turbulence models", *AIAA Journal*, Vol. 26, pp. 1299-1310.

[14] Kirillov, A.I., Ris, V.V., Smirnov, E.M., Zajtsev, D.K., 2001, "Numerical simulation of local heat transfer in rotating two-pass square channels", *Heat Transfer in Gas Turbine Systems. Annals of the New York Academy of Sciences*, Vol. 934, pp.456-463.

[15] Menter, F., Ferreira, J. C., Esch, T., Konno, B., 2003, "The SST turbulence model with improved wall treatment for heat transfer predictions in gas turbines", Proc. *Int. Gas Turbine Congress*, Tokyo, Japan, IGTC2003-TS-059.

[16] Smirnov, E.M., Zajtsev, D.K., 2004, "The finite-volume method in application to complex-geometry fluid dynamics and heat transfer problems", *Scientific-Technical Bulletin of the St.-Petersburg State Technical University*, No 2(36), pp. 70-81 (in Russian).

[17] Levchenya, A.M., Smirnov, E.M., Goryachev, V.D., 2010, "RANS-based numerical simulation and visualization of the horseshoe vortex system in the leading edge endwall region of a symmetric body", *Int. J Heat Fluid Flow*, Vol.31, pp. 1107-1112.